PHYSICAL REVIEW C **80**, 024302 (2009)

Decay of the $9/2^-$ isomer in ^{181}Tl and mass determination of low-lying states in ^{181}Tl, ^{177}Au, and ^{173}Ir

A. N. Andreyev,[1,7] S. Antalic,[2] D. Ackermann,[3] T. E. Cocolios,[1] V. F. Comas,[3] J. Elseviers,[1] S. Franchoo,[5] S. Heinz,[3] J. A. Heredia,[3] F. P. Heßberger,[3] S. Hofmann,[3,6] M. Huyse,[1] J. Khuyagbaatar,[3] I. Kojouharov,[3] B. Kindler,[3] B. Lommel,[3] R. Mann,[3] R. D. Page,[4] S. Rinta-Antila,[4] P. J. Sapple,[4] Š. Šáro,[2] P. Van Duppen,[1] M. Venhart,[1] and H. V. Watkins[4]

[1]*Instituut voor Kern-en Stralingsfysica, K. U. Leuven, University of Leuven, B-3001 Leuven, Belgium*
[2]*Department of Nuclear Physics and Biophysics, Comenius University, Bratislava, SK-84248, Slovakia*
[3]*GSI Helmholtzzentrum für Schwerionenforschung GmbH, D-64291 Darmstadt, Germany*
[4]*Department of Physics, Oliver Lodge Laboratory, University of Liverpool, Liverpool L69 7ZE, United KIngdom*
[5]*IPN Orsay, F-91406 Orsay Cedex, France*
[6]*Physikalisches Institut, J. W. Goethe-Universität, D-60054 Frankfurt, Germany*
[7]*School of Engineering and Science, University of the West of Scotland, Paisley, PA1 2BE, United KIngdom*

(Received 1 June 2009; published 4 August 2009)

A detailed spectroscopic study of the neutron-deficient isotope ^{181}Tl and the daughter of its α decay, ^{177}Au, has been performed in the complete fusion reaction $^{40}\mathrm{Ca} + ^{144}\mathrm{Sm} \rightarrow ^{184}\mathrm{Pb}^*$ at the velocity filter SHIP (GSI). The mass excess, excitation energy, and decay scheme of the isomeric 1.40(3) ms, $9/2^-$ intruder state in ^{181}Tl have been established for the first time. These results solve a long-standing puzzle of the unrealistically large reduced α-decay width of this isomer. Based on this, the previously unknown masses of the long-lived isomeric states in ^{177}Au and ^{173}Ir have been derived. In turn, it now allows the excitation energies of previously identified bands in ^{177}Au and ^{173}Ir to be deduced and compared with theoretical predictions. First measurements of α-decay branching ratios for $^{181}\mathrm{Tl}^m$ and $^{177}\mathrm{Au}^{m,g}$ are also reported.

DOI: 10.1103/PhysRevC.80.024302 PACS number(s): 23.60.+e, 21.10.Dr, 23.35.+g, 27.70.+q

I. INTRODUCTION

The region of very neutron deficient nuclei in the vicinity of the proton shell gap at $Z = 82$ and neutron midshell at $N = 104$ is well known for a prolific interplay between single-particle and collective nuclear structure effects [1–3]. To name a few examples specifically relevant to the present work, we mention the shape coexistence [1–4], shape staggering [5,6], and related phenomena in the broad region of the Pt-Rn isotopes and the persistence of high- and low-spin shell-model isomeric states. The occurrence of shell-model intruder states in the Tl ($Z = 81$) isotopes is another well-established phenomenon, see e.g. Refs. [7–10]. These complex and subtle effects lead to a variety of low-lying states with different structures that pose a stern test of theoretical models, while establishing the relative energies and, ideally, the masses of these structures is an important experimental challenge.

Different experimental methods have been applied in the past to study these effects, in-beam and/or isomeric γ-ray spectroscopy, β decay and reaction studies being the most widely used approaches [1–3]. However, by moving toward the more neutron-deficient nuclei, most of these methods cannot be applied and our knowledge of the nuclear structure in this region of nuclides becomes limited. Apart from the evident reduction of the production cross sections, this is partly due to either the lack of the stable targets (as required in the reaction studies), the limited sensitivity of the in-beam decay studies for nuclei with low production rates, or the strong reduction of the β-branching ratios as α decay becomes the dominant decay mode. Fortunately, α decay constitutes an ideal tool to identify selectively low-lying states in the very neutron deficient daughter nucleus, which have the same spin, parity, and configuration as in the α-decaying parent and that are often missed in the in-beam studies. Specifically in the region around the $Z = 82$ shell closure, the unhindered $\Delta L = 0$ α decay is a strong spectroscopic fingerprint for intruder states [10,11]. For example, our recent detailed α-decay studies of the odd-odd ^{184,186,188,190}Bi [12,13] and their daughter Tl isotopes provided detailed information on the systematic appearance of the normal and intruder states in this region of nuclei. Very importantly, in many cases α decay provides unique information on masses (based on the Q_α relationships) and excitation energies of the closely spaced and/or short-lived isomeric and ground states, which might currently not be accessible for experimental studies by other mass-measurement methods.

This work reports a dedicated spectroscopic study of the hitherto poorly understood nucleus ^{181}Tl ($N = 100$). Prior to our work, two α-decaying states were reported for this nucleus in three α-decay experiments [14–16], see Table I. The first one was a long-lived, presumably nearly spherical, $1/2^+$ state due to the $\pi 3s^{-1}_{1/2}$ configuration, which was interpreted as the ground state by analogy with the heavier odd-A Tl isotopes. Furthermore, again by analogy with the heavier odd-A Tl isotopes, a shorter-lived, $9/2^-$ intruder state presumably due to the $\pi 3s^{-2}_{1/2} \otimes 1h^{+1}_{9/2}$ configuration at an unknown excitation energy, was also suggested. Such $9/2^-$ states are known in the isotopes $^{183-201}$Tl [17]. Here we explicitly used the spherical shell-model language [18], in which such intruder states are treated as the 1p-2h proton particle excitations across the $Z = 82$ shell gap. In this approach their excitation energy is lowered due to the strong proton-neutron quadrupole-quadrupole interaction. As shown in Ref. [19], these states can equivalently be considered in the deformed mean-field approaches, where they are naturally understood

TABLE I. Comparison of α-decay energies E_α, half-life values $T_{1/2}$, and α-decay branching ratios b_α for ^{181}Tl and its daughter ^{177}Au from this experiment and from earlier studies. The literature data are shown only for the most recent studies, see Ref. [17] for more details. All I^π assignments are tentative.

Isotope, I^π	E_α (keV), $I_{\alpha,\mathrm{rel}}$ (%)	$T_{1/2}$ (ms)	b_α (%)	Reference
^{181}Tl^m, $9/2^-$	6578(7), 96.0(7)	1.40(3)	0.40(6)	This work
	6818(15), 1.4(7)	1.40(3)		This work
	6974(15), 2.6(7)	1.40(3)		This work
	6566(20)	2.7(10)		[14]
	6578(10)	1.4(5)		[16]
^{181}Tl^g, $1/2^+$	6181(7)		<10% [27]	This work
	6180	3400(600)		[15]
	6186(10)	3200(300)		[16]
^{177}Au^m, $11/2^-$	6124(7)	1000(200)	66(10)	This work
	6122(6)	1180(12)		[21]
	6118(9)	1300(200)		[25]
^{177}Au^g, $1/2^+$ or $3/2^+$	6161(7)	1530(70)	40(6)	This work
	6156(6)	1462(32)		[21]
	6154(10)			[25]

as based on the $9/2^-[514]$ Nilsson orbital that lies close to the Fermi surface at a moderate oblate deformation of $\epsilon_2 \sim 0.15$.

However, a completely puzzling observation from the earlier data was an apparent inconsistency between the relatively low α-decay energy of 6578(10) keV and the short half-life of 1.4(5) ms for the presumed $9/2^-$ isomeric state (using data from Ref. [16]). These decay properties contradict the expected α-decay systematics in this region [16]. Indeed, based on the reported data, an unrealistically large reduced α width of $\delta^2_\alpha(6578\ \mathrm{keV}) = 12(1)$ MeV can be calculated with the Rasmussen prescription [20] for this decay. This value is approximately three orders of magnitude larger than the reduced widths for unhindered α decays in this region.

In this work, we observed at least an order of magnitude more ^{181}Tl^m decays than any previous experiment. Combined with an advanced detection setup it allowed us to perform a significantly improved study of this nucleus and provide for the first time the correct and detailed decay scheme of ^{181}Tl. This resolves the above puzzle and establishes the mass, excitation energy, and configuration assignment for the short-lived $9/2^-$ isomeric state in this nucleus. This allows the evolution of the coexisting configurations to be traced even further beyond the neutron midshell at $N = 104$. Furthermore, for the first time the masses and excitation energies for the $11/2^-$ isomeric states in the daughter nuclei ^{177}Au and ^{173}Ir could be determined, which are not yet accessible for mass measurements by other methods due to their low production yields and a relatively small mass difference (~200 keV, see below) relative to the respective ground-state masses. The latter, in turn, fix the excitation energies of a few "floating" rotational bands that have been reported in these nuclei [17,21].

II. EXPERIMENTAL SETUP

The isotope ^{181}Tl was produced in the fusion-evaporation reaction $^{40}\mathrm{Ca} + {}^{144}\mathrm{Sm} \rightarrow {}^{184}\mathrm{Pb}^* \rightarrow {}^{181}\mathrm{Tl} + \mathrm{p2n}$. The typical intensity of the ^{40}Ca beam, provided by the UNILAC of GSI, Darmstadt, was ~400 pnA. The UNILAC macropulse had a total duration of 20 ms with a time structure of 5 ms "beam on" followed by a 15 ms "beam off" interval.

Eight ^{144}Sm targets, each of 96.4% enrichment and 350 μg/cm^2 thickness, were mounted on a wheel rotating synchronously with the UNILAC macropulsing. The targets were produced by evaporating the ^{144}SmF$_3$ material onto a carbon backing of 40 μg/cm^2 thickness and covered with a 10-μg/cm^2 carbon layer to increase the radiative cooling and reduce sputtering of the target material. Data were taken at several beam energies in the range of 177–229 MeV in the middle of the target, covering the energy range of the 2n-5n evaporation channels.

After separation by the velocity filter SHIP [22] the evaporation residues (ERs) were implanted into a 300-μm-thick, 35 × 80 mm^2 16-strip position-sensitive silicon strip detector (PSSD), where their subsequent particle decays were measured by using standard implantation techniques [23].

The α-energy calibration of the PSSD in the energy range of 5300–6800 keV was performed by using known α lines of the isotopes $^{176-182}$Hg, produced via the αxn channels of the studied reaction, and their daughters. A typical PSSD energy resolution of ~25 keV (FWHM) was achieved in the energy interval of 6000-7000 keV. Because α emission is a dominant decay mode of most of the nuclei produced in this reaction, the identification of nuclides was based on the observation of genetically correlated α-decay chains complemented with the excitation function measurements.

A large-volume fourfold segmented clover germanium detector was installed behind the PSSD to measure the energies of γ rays occurring within 5 μs of the detection of any particle decay in the PSSD. Three time-of-flight (TOF) detectors [24] were installed in front of the PSSD, allowing the reaction products to be distinguished from the scattered beam particles. In addition, decay events in the PSSD could be distinguished from the implantation events by requiring an anticoincidence condition between the signals from the PSSD and from at least one of the TOF detectors.

III. EXPERIMENTAL RESULTS

Table I summarizes the decay properties of some of the isotopes studied in this work in comparison with the previously known data. Our data were deduced by using ER-α_1 and ER-α_1-α_2 correlation analyses with different optimal correlation time and energy conditions for each isotope, only some of which will be discussed in the text.

A. α decay of ^{181}Tl^m

Figure 1(a) shows a part of the energy spectrum of α decays collected within a time interval of 6 ms after an ER implantation in the PSSD, which was specifically selected

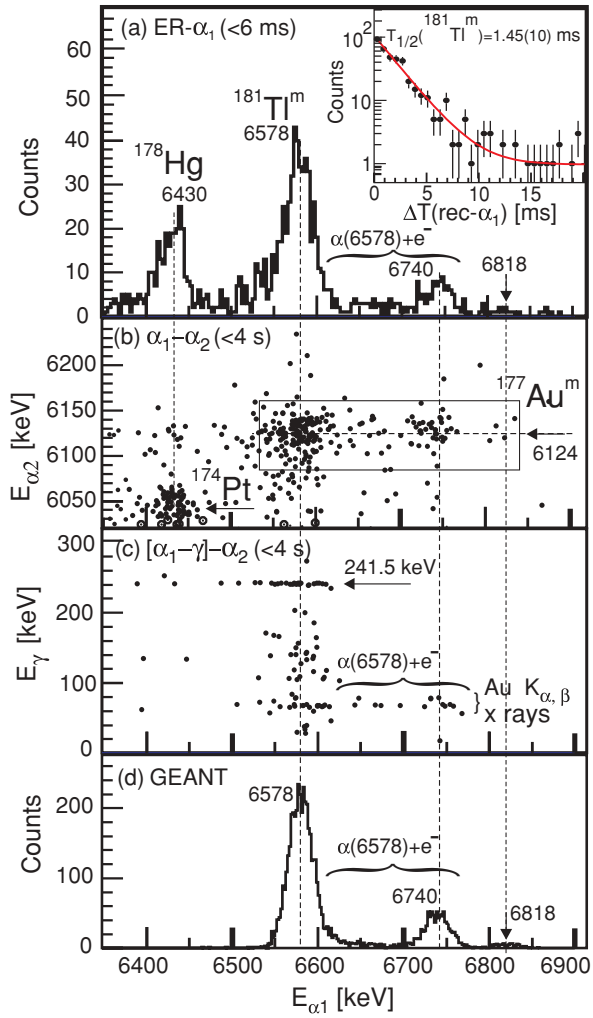

FIG. 1. (Color online) (a) A part of the α_1-energy spectrum for the reaction ^{40}Ca + ^{144}Sm → ^{184}Pb* registered in the PSSD within 6 ms after an ER implantation. The curly bracket denotes the events due to the α(6578 keV)-e^- summing events, see the text for details. α-decay energies are given in keV. The inset shows the time difference between the ER and a subsequent α decay in the region of 6540–6830 keV (^{181}Tl^m). The fit by an exponential function with a constant background is shown by a solid line. (b) the α_1-α_2 correlation plot for the α_1 decay from panel (a), measured within the time interval of $\Delta T(\alpha_1\text{-}\alpha_2) \leqslant 4$ s. (c) The prompt E_α-E_γ coincidence spectrum for α_1 events from (b); (d) the result of GEANT simulations for the coincident α(6578 keV)-γ and α(6578 keV)-e^- decays of ^{181}Tl^m, see text for details.

to enhance the short-lived isotope ^{181}Tl^m. The two strongest peaks at 6430(8) keV and 6578(7) keV are due to known decays of ^{178}Hg and ^{181}Tl^m, respectively. Both values are in very good agreement with those previously reported (see Table I for ^{181}Tl^m), which confirms our energy calibration procedure of the PSSD. The group at 6740(20) keV and a weak group at 6818(15) keV will be discussed below.

Figure 1(b) shows the two-dimensional plot of α_1-α_2 correlations for the α_1 decays from Fig. 1(a) for the time interval of $\Delta T(\alpha_1\text{-}\alpha_2) \leqslant 4$ s. A weak group of known α_1(^{178}Hg)-α_2(^{174}Pt) correlations is present in the spectrum. We note, however, that by using the ER-α_1-α_2 correlation analysis with the longer ER-α_1 time condition suitable for the ∼260-ms isotope ^{178}Hg [17], we collected ∼10^4 correlated ^{178}Hg-^{174}Pt events. This allowed us to deduce the α-decay branching ratio of $b_\alpha(^{174}\text{Pt}) = 67(2)\%$, which is in good agreement with but more precise than the value of $b_\alpha = 67(6)\%$ from the study [25]. However, both values differ from the value of $b_\alpha = 83(5)\%$ reported in an earlier study [26].

Now we will discuss the three groups of correlated decays with the α_1 energies within the 6540- to 6830-keV interval, denoted by the rectangle in Fig. 1(b), including a weak group of four events with $E_{\alpha 1} = 6818(15)$ keV. Apart from having the same ER-α_1 time behavior (see below), all of them correlate with the 6124(7)-keV α decay of ^{177}Au^m. Therefore, these three groups must originate from the decay of ^{181}Tl^m. We note that our α-decay energy for ^{177}Au^m is in good agreement with the value of 6122(6) keV from the study [21]. Based on the ER-α_1 (6540–6830 keV) correlation analysis, a half-life value of 1.45(10) ms was deduced from the α decays of ^{181}Tl^m, see inset to Fig. 1(a).

Figure 1(c) shows the two-dimensional α_1-γ spectrum for α_1 events from Fig. 1(b), measured within the time interval of $\Delta T(\alpha\text{-}\gamma) \leqslant 5$ μs. We interpret the α(6578-keV)-γ (241.5(3)-keV) group in this spectrum, which has never been seen in previous experiments, as due to the fine-structure α decay of ^{181}Tl^m to the previously known $9/2^-$ excited state in ^{177}Au^m [21]. Here we assume that the 241.5(3)-keV transition is the same as the 240.8-keV $M1$ ($9/2^- \rightarrow 11/2^-$) decay seen in the in-beam work [21]. This readily explains the weak 6818(15)-keV α decay seen in Figs. 1(a) and 1(b) as the full-energy "crossover" transition to the $11/2^-$ isomeric state of ^{177}Au^m, as shown in the decay scheme in Fig. 2.

The K conversion of the 241.5-keV $M1$ transition in the daughter isotope ^{177}Au readily explains the presence in Fig. 1(a) of both the 6740-keV peak and the events between the 6578-keV and the 6740-keV peaks. Indeed, the internal conversion of this transition results mainly in the K-conversion electrons ($\alpha_K(241.5, M1) = 0.495$ [28]) with an electron energy of ∼161 keV (the K/L ratio is ∼6 [28]). Therefore, depending on the scattering angle of these electrons, their energy will be either fully or partially summed in the PSSD with the energy of the 6578-keV α decay. Clearly, the full-energy summing produces the 6740-keV peak seen in our spectra, while the partial energy summing (when the electron escapes from the PSSD) produces the events between the 6578- and 6740-keV peaks. These events are denoted as "α(6578 keV)+e^-" in Fig. 1. Such events must be in coincidence with the Au $K_{\alpha,\beta}$ x rays, which is indeed seen in Fig. 1(c).

To confirm this scenario, we performed GEANT Monte Carlo simulations with the dedicated code, developed for the SHIP detection system, see Ref. [29]. The simulations were performed according to the decay scheme shown in Fig. 2. To show the most salient features, we neglected the L-conversion electron summing, as it is relatively weak and its inclusion does not change our conclusions. The result of the simulations is shown in Fig. 1(d) and clearly demonstrates that the shape and intensity ratios of the peaks in the experimental and simulated

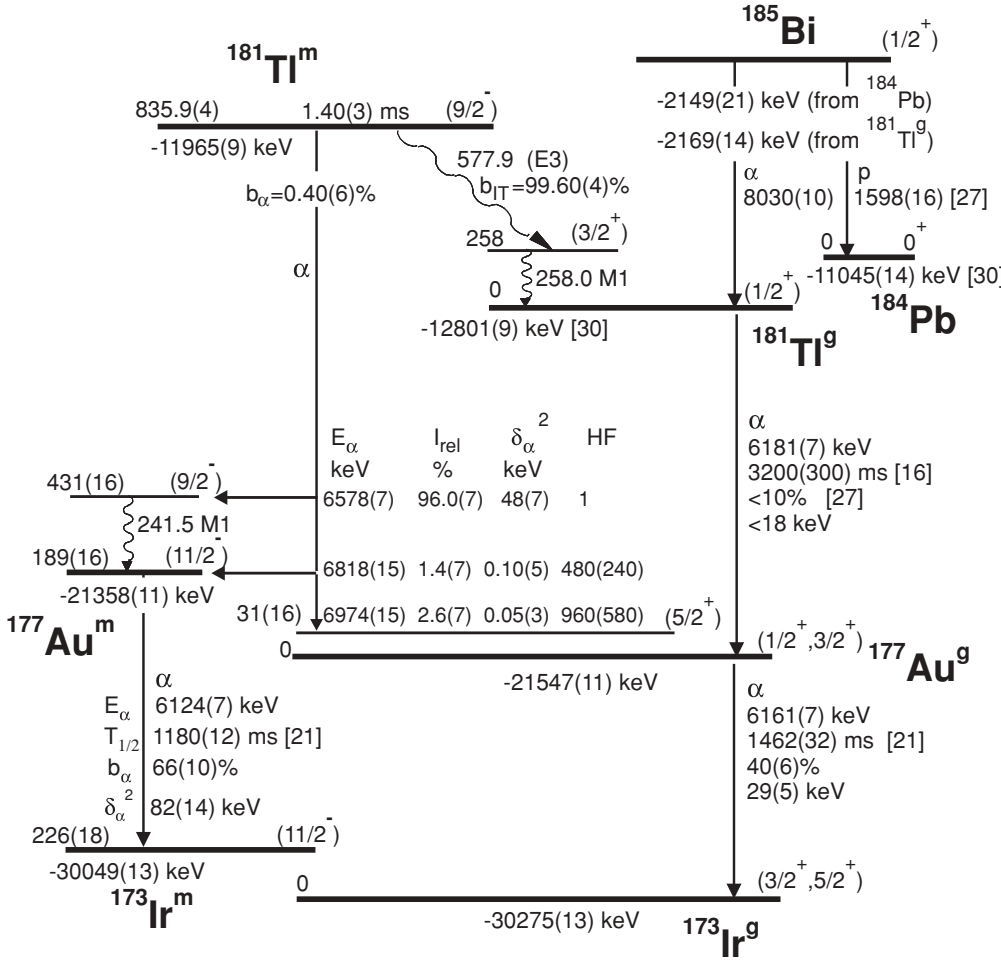

FIG. 2. Decay scheme of ^{181}Tl^m and of some of the daughter nuclides deduced in our work. Shown are α-decay energies E_α, half-life values $T_{1/2}$, relative intensities $I_{\rm rel}$ (for ^{181}Tl^m only), α-decay branching ratios b_α, and reduced α-decay widths δ^2_α. The reduced α-decay widths were calculated with the Rasmussen prescription [20] by assuming $\Delta L = 0$ decays. The hindrance factors HF$_\alpha$ for ^{181}Tl^m were calculated relative to the 6578-keV decay, for which HF$_\alpha = 1$ was assumed. For the values that were not measured in this work, or for which more precise data exist in the literature, the references are given to the original studies. The "reference" mass excess values of ^{181}Tl^g and of ^{184}Pb are taken from Ref. [30]. All other mass excess values are derived in this work, see Sec. IV.

spectra are similar. This confirms the α-decay scheme of ^{181}Tl^m and all our assumptions discussed above.

One more weak α decay of ^{181}Tl^m with approximately 20 counts in the ER-α_1 analysis (not shown in Fig. 1) was observed at $E_\alpha = 6974(15)$ keV. The deduced half-life of 1.3(2) ms for these decays confirms their origin as from ^{181}Tl^m. We tentatively placed this decay as feeding the $E^* = 31(16)$ keV $(5/2^+)$ state in ^{177}Au^m, see Fig. 2 and the discussion in Sec. IV.

By comparing the number of ER-α_1(6540–6830 keV) events from Fig. 1(a) and the number of ER-α_1(6540–6830 keV)-α_2(6124 keV) events from Fig. 1(b) (corrected for the limited correlation time interval), the α-decay branching ratio of $b_\alpha(^{177}\text{Au}^m) = 66(10)\%$ was deduced for the first time.

B. γ decay of ^{181}Tl^m

As already mentioned in the Introduction, by assuming an α-decay branching ratio of $b_\alpha = 100\%$ for the 6578-keV decay of ^{181}Tl^m, an unrealistically large reduced α-decay width of $\delta^2_\alpha(6578\ \text{keV}) = 12(1)$ MeV is obtained with the Rasmussen prescription [20] for a $\Delta L = 0$ α decay. From the comparison of this value with the typical values of $\delta^2_\alpha \sim 40$–80 keV for unhindered decays in this region, a conclusion can be drawn that the 6578-keV α decay must represent only a small fraction of the total decay width of ^{181}Tl^m. Therefore, a search was performed for the internal transition (IT) branch of ^{181}Tl^m to the states above the $1/2^+$ ground state in ^{181}Tl. Such internal transition branches are well known, for instance, in the isotopes $^{193-201}$Tl [17].

To perform this search, we used the fact that the UNILAC "macropulse" in our experiment had the time structure of 5 ms "beam on" and 15 ms "beam off," thus the ERs were implanted in the PSSD only during the "beam on" interval. During the "beam off" interval, only the decay of ERs happened. Clearly, if the internal transition branch of the short-lived 1.40 ms ^{181}Tl^m exists, the corresponding internal transition γ rays will happen mostly in the "beam on" interval and to some degree

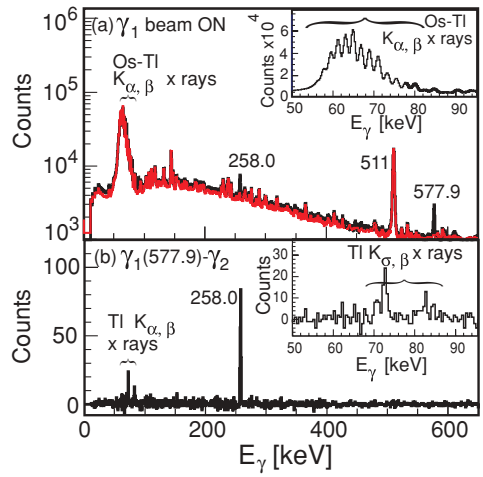

FIG. 3. (Color online) a) γ-ray spectra collected within the "beam on" time interval of 5 ms (in black) and within the time interval of 10–20 ms during the "beam off" period (red) of the UNILAC macro pulse. The spectra are normalized on the intensity of the 511-keV γ line. Some γ lines are marked by their energies in keV. The inset shows the 50- to 95-keV part of the "beam on" spectrum; (b) Background-subtracted γ_1-γ_2 coincidence spectrum with a gate on the 577.9-keV γ ray. The inset shows the 50- to 95-keV part of the full spectrum.

within a limited time interval of a few milliseconds after the end of the "beam on" interval.

Therefore, the γ-ray spectrum registered within the "beam on" interval of 5 ms is shown in Fig. 3(a) in black, while the spectrum for the "beam off" time interval within 10–20 ms is shown in red. The latter time interval was chosen to produce a pure "background" γ-ray spectrum, in which the contribution of the γ rays of ^{181}Tl^m must be negligible. Both spectra were normalized on the intensity of the 511-keV peak, which clearly originates from longer-lived activities. The spectra show the presence of strong groups of $K_{\alpha,\beta}$ x rays of long-lived Os-Tl isotopes [see inset to Fig. 3(a)], which are abundantly produced both directly in the reaction and also as the decay products of the implanted activities. Figure 3(a) demonstrates that the two peaks at 258.0(3) keV and 577.9(3) keV are present only in the "beam on" period.

Figure 3(b) shows the background-subtracted γ_1-γ_2 coincidence spectrum with a gate on the 577.9-keV γ_1 ray occurring within the "beam on" interval only. As the "background" spectrum we used the spectrum with a gate on the same 577.9-keV transition, but within the "beam off" interval, when this decay does not occur as shown by the corresponding spectrum in Fig. 3(a). The presence in Fig. 3(b) of the 258.0-keV transition unambiguously proves that the 258.0- and 577.9-keV γ rays are in coincidence with each other. Furthermore, the excitation function for the γ(258.0 keV)-γ(577.9 keV) coincident events (not shown in this work) has the same shape and beam energy dependence as the excitation function for the 6578-keV decay of ^{181}Tl^m, which proves that this cascade happens in a nucleus with $A = 181$. The expanded part of Fig. 3(b) is also shown in the inset, where the Tl $K_{\alpha,\beta}$ x rays can be seen. Taken together with the excitation function analysis, this proves that the 258.0- to 577.9-keV γ cascade happens in ^{181}Tl. By comparing the number of observed Tl $K_{\alpha,\beta}$ x rays with the number of 258.0-keV γ decays (after correcting for γ-ray detection efficiency), a K-conversion coefficient of $\alpha_K(258.0\ \text{keV}) = 0.49(8)$ was deduced. This establishes a predominant $M1$ multipolarity for the 258.0-keV decay, as the theoretical value is $\alpha_K = 0.486$ [29].

A similar analysis was performed for the γ_1-γ_2 coincidences with a gate on the 258.0-keV transition. The only peak seen in the spectrum was at 577.9 keV with a very weak group of Tl K x rays. This allowed us to estimate an upper limit for the K conversion coefficient of $\alpha_K(577.9\ \text{keV}) \leqslant 0.1$, which is consistent with an $E3$ multipolarity assignment ($\alpha_K(\text{theor}) = 0.036$ [28]) as suggested below.

To strengthen our interpretation, we determined the half-life values for the 577.9- and 258.0-keV decays. As an example, Fig. 4 shows the intensity distribution of the 577.9-keV transition as a function of time within the 20 ms of the UNILAC beam structure. As expected for a short-lived activity, one sees both the "grow-in" part in the beginning of the "beam on" interval and also the "decay-out" part right after the stop of the "beam on" interval. The half-life of 1.40(8) ms was determined for the 577.9-keV decay by fitting the "decay-out" part of the spectrum with an exponential function and a constant background in the "beam off" time interval of 5–20 ms in Fig. 4(a). By using the same method, a similar half-life value of 1.40(7) ms was deduced for the 258.0-keV transition. Finally, based on combined statistics for the 258.0- and 577.9-keV γ rays, a half-life value of 1.40(3) ms was derived, which we adopt as the half-life for the isomer ^{181}Tl^m. The half-life value of 1.45(10) ms for the much weaker α-decay branch of ^{181}Tl^m is in good agreement with the above value. Therefore, based on all above arguments, we assign the 258.0- to 577.9-keV γ cascade to the internal transition of ^{181}Tl^m.

The α-decay and IT branching ratios were deduced by comparing the number of α-γ(241.5 keV) coincident events, corrected for the ∼50% PSSD efficiency for the full energy

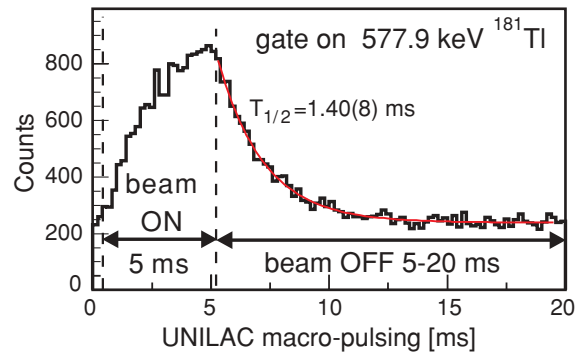

FIG. 4. (Color online) Time distribution of the 577.9-keV γ ray of ^{181}Tl^m within the 20-ms macro-pulse of UNILAC. The time intervals used as "beam on" and "beam off" are shown by arrows. The fit performed by an exponent with a constant background is shown by the red line.

α decays, and the number of isomeric 258.0-keV γ decays resulting from the IT decay and measured during the "beam on" interval from Fig. 3(a). The main advantage of this method is that both γ-ray transitions are of the same $M1$ multipolarity and have similar energies. Therefore, both their conversion coefficients and γ-ray efficiencies cancel out in this method, while the experimental uncertainty will only be defined by the relatively small number of α-γ coincident events. Based on this comparison, branching ratios of $b_\alpha = 0.40(6)\%$ and $b_{\rm IT} = 99.60(6)\%$ were deduced. The reduced α-decay width for the 6578-keV decay, calculated with this branching ratio is 48(7) keV, which is only slightly smaller than the reduced widths for the unhindered $0^+ \rightarrow 0^+\alpha$ decays in the neighboring even-even isotopes ^{182}Pb [$\delta^2_\alpha = 61(7)$ keV] and ^{180}Hg [$\delta^2_\alpha = 74(8)$ keV]. This confirms the unhindered nature of the 6578-keV decay, which then must connect the states with the same spin, parity, and configuration in the parent and daughter nuclei. In contrast to this, the "crossover" 6818-keV decay is strongly hindered [$\mathrm{HF}_\alpha = 480(240)$] relative to the 6578-keV decay, which proves that the daughter state in ^{177}Au fed by this decay must have a different configuration to that of $^{181}\mathrm{Tl}^m$.

In our study we also observed ~3000 α_1 (6181 keV)-α_2(6161 keV) correlated events due to the decay chain $^{181}\mathrm{Tl}^g \rightarrow {}^{177}\mathrm{Au}^g$ of the $1/2^+$ ground state of ^{181}Tl. The measured α-decay energies of $^{181}\mathrm{Tl}^g$ and of $^{177}\mathrm{Au}^g$ and the half-life value of $^{177}\mathrm{Au}^g$ are in good agreement with the previously known values, see Table I. However, due to the high implantation rate of ERs, no half-life value could be deduced for the long-lived $^{181}\mathrm{Tl}^g$. However, by using the α-α correlation analysis, we deduced the previously unknown α-branching ratio of $b_\alpha(^{177}\mathrm{Au}^g) = 40(6)\%$. In Table I and Fig. 2 we show our measured α-decay data together with the literature data from Refs. [17,21,27] for those cases where the corresponding values could not be measured in our work.

IV. DISCUSSION

The intruder $9/2^-$ isomeric states are well known in the odd-A isotopes $^{183-201}$Tl [8,33], see Fig. 5. Within the shell-model approach they are readily understood as due to the proton excitation from the $1/2^+[\pi 3s^{-1}_{1/2}]$ ground state to the $9/2^-[\pi 1h_{9/2}]$ orbital above the shell gap at $Z = 82$. In the deformed mean-field approaches, these states are usually treated as based on the $9/2^-[514]$ Nilsson orbital that lies close to the Fermi surface at a moderate oblate deformation of $\epsilon_2 \sim 0.15$. In the past, the decay of these states in some of the heavier isotopes, e.g., $^{193-201}$Tl has been studied in detail, see Ref. [17]. In these nuclei, the decay proceeds predominantly, if not exclusively, via an $E3$ internal transition decay to the lower-lying $3/2^+[\pi 2d^{-1}_{3/2}]$ excited state, as can be seen from Fig. 5 where these states are also shown. A typical value of $B(E3) \sim 0.01$ W.u. was deduced for the $9/2^- \rightarrow 3/2^+$ decays in the isotopes $^{195-201}$Tl.

In contrast to this, though the excitation energies of the $9/2^-$ states in the lighter isotopes $^{183-193}$Tl are known, the detailed decay paths of these states have not so far been established. This is partly because in some of the isotopes, e.g., in ^{189,191}Tl

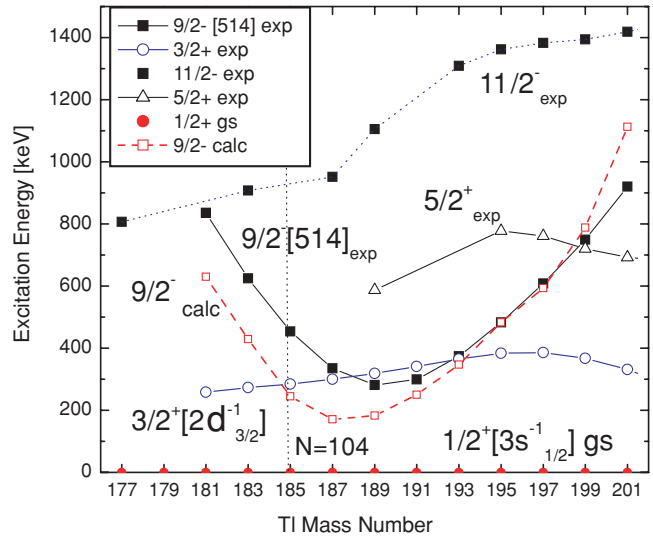

FIG. 5. (Color online) Experimental excitation energies of selected excited $3/2^+$, $9/2^-$, $11/2^-$, and $5/2^+$ states in the odd-A Tl isotopes, relative to the respective $1/2^+$ ground states [8,17,32]. The experimental uncertainties are usually smaller than the symbol sizes and therefore not shown. The calculations for the $9/2^-$ states have been performed as described in Ref. [27]. The lines connecting the experimental $11/2^-$ and $5/2^+$ states are shown to guide the eye.

the $9/2^-$ states are below the $3/2^+$ states, thus their decay would proceed via very slow $M4$ transitions directly to the $1/2^+$ ground state or, possibly, via β^+/EC decay. Another reason is that by moving toward the most neutron-deficient nuclei the production rate becomes very low, which often prohibits performing detailed studies. In this respect, our new results for ^{181}Tl provide a unique example of a detailed spectroscopic study of the newly established $9/2^-$ intruder state in this nucleus, lying beyond the neutron midshell at $N = 104$.

First of all, by analogy with the heavier Tl isotopes, we assign the 258.0-keV $M1$ transition as de-exciting the newly identified $3/2^+$ excited state in ^{181}Tl. As seen from Fig. 5, this state follows well the smooth and nearly constant energy systematics of such states in the isotopes $^{183-201}$Tl. These states are understood as due to the proton excitation from the $2d_{3/2}$ single-particle orbital to fill the $3s_{1/2}$ orbital. However, we notice that in the heavier odd-A isotopes $^{187,193-199}$Tl, the corresponding de-exciting $2d_{3/2} \rightarrow 3s_{1/2}$ γ-ray transitions have typically a large $M1 + E2$ mixing ratio, of the order of $\delta(M1 + E2) \sim 1.5$–2 [17], most probably, due to their expected dominant $\Delta L = 2$ character within the spherical shell model. For example, a mixing ratio of $\delta(M1 + E2) = 2.0^{+0.5}_{-0.3}$ was deduced in ^{187}Tl. However, in the midshell nucleus ^{185}Tl ($N = 104$), a lower mixing ratio of $\delta(M1 + E2) = 0.91(20)$ is known [17]. Futhermore, our data indicate a predominant $M1$ character for the 258-keV $2d_{3/2} \rightarrow 3s_{1/2}$ transition in ^{181}Tl. Together with the ^{185}Tl data, this might indicate that a change of the mixing ratio for the $2d_{3/2} \rightarrow 3s_{1/2}$ transition toward a more pure $M1$ character sets in from ^{185}Tl on.

Based on the $3/2^+$ assignment for the 258-keV level, the feeding 577.9-keV transition must be of $E3$ multipolarity,

de-exciting the $9/2^-$ state. The $E3$ multipolarity assignment is also confirmed by the deduced value of $B(E3, 577.9\ \text{keV}) = 0.022$ W.u. for this transition, which is comparable to the $B(E3)$ values for the $9/2^- \rightarrow 3/2^+$ decays in $^{195-201}$Tl.

This establishes for the first time the excitation energy of the $9/2^-$ state in ^{181}Tl as 835.9(4) keV, see Fig. 2. It is important to notice that although the excitation energy of the $11/2^-$ state is not yet known in ^{181}Tl, it must lie above the $9/2^-$ state, similar to the isotopes $^{183-203}$Tl where such states are known, see Fig. 5. Otherwise, the $9/2^-$ state would most probably decay by a much faster $M1$ decay.

Within the spherical shell-model description, it is expected that the excitation energy of the intruder states should follow a parabolic trend as a function of the neutron number with a minimum in the vicinity of the neutron midshell at $N = 104$. This is because the dominant underlying mechanism involves the residual quadrupole-quadrupole proton-neutron interaction between valence protons and neutrons, see Ref. [18]. As the number of valence neutrons is the largest for the midshell nuclei, in our case for $N = 104$, the minimum of the parabola would be expected around ^{185}Tl. This is clearly not the case in Fig. 5, which shows that the experimental minimum for the $9/2^-$ states happens already in ^{189}Tl. Furthermore, the parabola is clearly asymmetric, with a steeper increase of the excitation energy by moving toward the lighter nuclei. Both these facts suggest that more subtle interactions are involved on top of the quadrupole proton-neutron residual interaction.

We also performed potential-energy surface calculations for the $9/2^-$ states in the $^{181-201}$Tl isotopes, see Fig. 5 and a detailed description in Ref. [27]. A very good agreement between the calculated and experimental data was achieved for the heavier isotopes $^{191-201}$Tl, while a moderate deviation of $\sim$200 keV appears for the lighter nuclei. Despite this, both the shifted minimum and asymmetric parabolic behavior are also reproduced by the calculations. Further theoretical studies are necessary to address these observations.

By extrapolating the parabolic trend of the $9/2^-$ states to ^{179}Tl, an expected excitation energy of $E^*(9/2^-) \sim 1170$ keV can be estimated in this nucleus. This excitation energy would already be by $\sim$300–400 keV higher than the expected position of the $11/2^-$ state in ^{179}Tl, thus the $9/2^-$ in this nucleus is not expected to be isomeric. This is actually what was suggested in the earlier α decay studies of ^{179}Tl [16,33] and was recently confirmed in our more detailed work on this nucleus [34].

By using the known mass excess of $\Delta M = -12801(9)$ keV from Ref. [32] (cf. to the value of $\Delta M = -12802(10)$ keV from the recent ISOLTRAP measurement [35]) and the excitation energy of 835.9 keV, we deduce the previously unknown mass excess of $\Delta M = -11965(9)$ keV for the short-lived 1.40 ms $9/2^-$ isomer in ^{181}Tl, see Table II.

This, along with the new detailed α-decay scheme of ^{181}Tl^m and confirmed α decay of its daughter ^{177}Au^g allows us to deduce the previously unknown masses of ^{177}Au^m [$\Delta M = -21358(11)$ keV] and ^{173}Ir^m[$\Delta M = -30049(13)$ keV], see Table II. In turn, this allows us to establish the absolute excitation energies of these $11/2^-$ isomers relative to the corresponding ground states in these nuclei and the values are shown in Fig. 2. For example, it now becomes possible to determine the absolute excitation energy of the previously known "floating" bands in ^{177}Au, observed in Ref. [21]. Namely, the previously unknown excitation energy of the $(5/2^+)$ state denoted as "x" in the decay scheme of ^{177}Au in Fig. 1 of the study [21] is now established as $x = E^*(5/2^+) = 31(16)$ keV, see Fig. 2.

TABLE II. Mass excess values from our measurement and from AME2003 [30]. The tabulated mass excess values [30] of ^{181}Tl^g[$\Delta M = -12801(9)$ keV] and of ^{184}Pb [$\Delta M = -11045(14)$ keV] were used as reference values to derive all other data.

Nuclide	Our value	AME2003 [30]
^{181}Tl^m	−11965(9)	
^{181}Tl^g		−12801(9)
^{177}Au^m	−21358(11)	
^{177}Au^g	−21547(11)	−21550(13)
^{173}Ir^m	−30049(13)	
^{173}Ir^g	−30275(13)	−30272(14)
^{185}Bi	−2149(21)[a]	−2210(50)
^{185}Bi	−2169(14)[b]	−2210(50)

[a]Deduced from the tabulated mass excess of ^{184}Pb [30].
[b]Deduced from the tabulated mass excess of ^{181}Tl^g [30].

Based on our measured α-decay energies, the mass excess values for the isotopes ^{177}Au^g and ^{173}Ir^g were also deduced. They are compared in Table II with the data from AME2003 [30]. The energy of the 6974-keV α decay of ^{181}Tl^m is equal within the experimental uncertainty to the energy difference between the $9/2^-$ state of ^{181}Tl^m and the $5/2^+$ excited state at 31(16) keV in ^{177}Au. That is why we placed the 6974-keV decay as shown in Fig. 2. The hindrance factor of $\text{HF}_\alpha = 960(580)$ (see Fig. 2), which is larger than that for the 6818-keV $9/2^- \rightarrow 11/2^-$ α decay, is in agreement with this suggestion.

Finally, we notice that the reduced α width ($\delta^2_\alpha < 18$ keV) for the 6181-keV α decay of ^{181}Tl^g is lower by at least a factor of 2 relative to the reduced α widths for the unhindered $0^+ \rightarrow 0^+$ α decays in this region. This is also seen from the comparison with other, presumably unhindered, α decays shown in Fig. 2, for which the reduced α widths are in the region of 30–80 keV. This hindrance suggests different parent and daughter configurations for the states, connected by the 6181-keV decay. In the literature, two possible configurations of $1/2^+[411]$ (oblate deformation) or $3/2^+[402]$ (prolate deformation) Nilsson configurations were tentatively discussed for ^{177}Au^g, see Ref. [17]. Unfortunately, based on the observed moderate hindrance for the 6181-keV decay, which proceeds from the nearly spherical $3s_{1/2}$ state of ^{181}Tl^g, no distinction between the two possible assignments for ^{177}Au^g can yet be made.

For completeness, we deduced the mass excess value for ^{185}Bi by using the previously known masses of its daughter products ^{181}Tl (after α decay) and ^{184}Pb (after proton decay) [30] and known α and proton decay energies of ^{185}Bi [27]. The resulting two values are shown in Fig. 2 and Table II.

They are consistent with each other within the experimental uncertainties, but differ slightly from the less precise estimated value of –2210(50) keV, deduced from systematics and quoted presently in AME2003 [30].

V. CONCLUSIONS

A detailed spectroscopic study of the isotope ^{181}Tl was performed in the complete fusion reaction of ^{40}Ca ions with the ^{144}Sm target. The high statistics collected in our experiment, along with the application of the method of delayed γ coincidences at a recoil separator allowed us to establish unambiguously both the weak 0.40(6)% α decay and the dominant internal transition branches. The cascade of the 258.0 keV–577.9 keV γ rays due to the internal transition decay of the $9/2^-$ isomeric state in ^{181}Tl determined for the first time its excitation energy. It extends the nearly parabolic trend of the excitation energy of such isomeric states to the neutron number $N = 100$ and explains the absence of such $9/2^-$ isomeric states in the lighter isotopes ^{177,179}Tl, in which the $9/2^-$ state is expected to be situated above the $11/2^-$ state.

The masses of the long-lived α-decaying isomers in ^{181}Tl, ^{177}Au, and ^{173}Ir were deduced for the first time. For the last two nuclei, these results allowed the absolute excitation energies of a few previously known "floating" bands to be established. The relative energies of these states deduced in this work fit in well with the systematic behavior of Tl isotopes. Nevertheless, significant features such as the divergence of calculated and measured values for $9/2^-$ states in lighter isotopes will require further theoretical study.

ACKNOWLEDGMENTS

We thank the UNILAC staff for providing the stable and high-intensity ^{40}Ca beams. This work was supported by FWO-Vlaanderen (Belgium), GOA/2004/03 (BOF-K.U.Leuven) and the "Interuniversity Attraction Poles Programme–Belgian State Belgian Science Policy" (BriX network P6/23), by the European Commission within the Sixth Framework Programme through I3-EURONS (Contract RII3-CT-2004-506065) and by the UK Science and Technology Facilities Council. S. Antalic and Š. Šáro were supported by the Slovak Research and Development Agency under Contract No. APVV-20-006205.

[1] K. Heyde *et al.*, Phys. Rep. **102**, 291 (1983).
[2] J. L. Wood *et al.*, Phys. Rep. **215**, 101 (1992).
[3] R. Julin, K. Helariutta, and M. Muikku, J. Phys. G: Nucl. Part. Phys. **27**, R109 (2001).
[4] A. N. Andreyev *et al.*, Nature **405**, 430 (2000).
[5] J. Bonn *et al.*, Phys. Lett. **B38**, 308 (1972).
[6] G. Ulm *et al.*, Z. Phys. A **325**, 247 (1986).
[7] A. J. Kreiner, C. Baktash, G. Garcia Bermudez, and M. A. J. Mariscotti, Phys. Rev. Lett. **47**, 1709 (1981).
[8] E. Coenen, K. Deneffe, M. Huyse, P. Van Duppen, and J. L. Wood, Phys. Rev. Lett. **54**, 1783 (1985).
[9] M. Huyse *et al.*, Phys. Lett. **B201**, 293 (1988).
[10] P. Van Duppen *et al.*, Nucl. Phys. **A529**, 268 (1991).
[11] M. Huyse and P. Van Duppen, Hyperfine Interact. **132**, 141 (2001).
[12] A. N. Andreyev *et al.*, Eur. Phys. J. A **18**, 39 (2003).
[13] A. N. Andreyev *et al.*, Eur. Phys. J. A **18**, 55 (2003).
[14] J. R. H. Schneider, Ph.D. thesis, GSI report, GSI-84-3 (unpublished, 1984).
[15] V. A. Bolshakov *et al.*, in *Nuclei Far from Stability/Atomic Masses and Fundamental Constants 1992*, IOP Conf. Proc. No. 132 (Institute of Physics and Physical Society, Bristol, 1993), p. 743.
[16] K. S. Toth *et al.*, Phys. Rev. C **58**, 1310 (1998).
[17] Evaluated Nucelar Structure Data File (ENSDF), http://www.nndc.bnl.gov/ensdf/.
[18] K. Heyde *et al.*, Nucl. Phys. **A484**, 275 (1988).
[19] K. Heyde *et al.*, Phys. Lett. **B218**, 287 (1989).
[20] J. O. Rasmussen, Phys. Rev. **113**, 1593 (1959).
[21] F. G. Kondev *et al.*, Phys. Lett. **B512**, 268 (2001).
[22] G. Münzenberg *et al.*, Nucl. Instrum. Methods **161**, 65 (1979).
[23] S. Hofmann *et al.*, Z. Phys. A **291**, 53 (1979); S. Hofmann and G. Münzenberg, Rev. Mod. Phys. **72**, 733 (2000).
[24] S. Saro *et al.*, Nucl. Instrum. Methods A **381**, 520 (1996).
[25] R. D. Page *et al.*, Phys. Rev. C **53**, 660 (1996).
[26] E. Hagberg *et al.*, Nucl. Phys. **A318**, 29 (1979).
[27] A. N. Andreyev *et al.*, Phys. Rev. C **69**, 054308 (2004).
[28] T. Kibédi *et al.*, Nucl. Instrum. Methods A **589**, 202 (2008). Conversion coefficients calculator BrIcc v2.2a, http://wwwrsphysse.anu.edu.au/nuclear/bricc/.
[29] A. N. Andreyev *et al.*, Nucl. Instrum. Methods A **533**, 409 (2004).
[30] G. Audi, A. H. Wapstra, and C. Thibault, Nucl. Phys. **A729**, 337 (2003).
[31] R. B. Firestone *et al.*, *Table of Isotopes, 8th Edition* (John Wiley & Sons, Inc., New York, 1996).
[32] J. Sauvage *et al.*, Eur. Phys. J. A **39**, 33 (2009).
[33] G. L. Poli *et al.*, Phys. Rev. C **59**, R2979 (1999).
[34] A. N. Andreyev *et al.*, Phys. Rev. C **79**, 064320 (2009).
[35] C. Weber *et al.*, Nucl. Phys. **A803**, 1 (2008).